Evidence for general downward trend of the SXR solar flare activity in the last decades

Boris Komitov[1], Peter Duchlev[1], Kaloyan Penev[2]
[1] Institute of Astronomy and NAO, Bulgarian Academy of Sciences, 1784 Sofia, Tsarigradsko Chaussee blvd. 72
[2] Department of Astrophysical Sciences, Princeton University, 4 Ivy Lane, Peyton Hall, Princeton, NJ 08544, USA
b_komitov@sz.inetg.bg
(Submitted on 14.04.2015; Accepted on 15.05.2015)

Abstract. On the basis of the overall GOES satellites data for the period 1976–2014 AD multiple regression models of three detached "synthetic" series were built. They are consisted of the monthly numbers of soft X-ray flares (SXR) separately for the classes C, M, and X for the epoch 1968–2014 AD. The monthly numbers of radiobursts at three frequencies (609, 8800, and 15400 MHz) and the radio flux at 2800 MHz ($F10.7$) are used as inputs. Very strong relationships are found (correlation coefficients R are from 0.79 to 0.92 and Snedekor-Fisher's F parameter is in the range of 2.6–6.4). It appears that the older SOLRAD satellite data (1968–1974 AD) are not precise enough, regarding especially to the C-class flares. Some features of residuals between the obtained regression models and original data are analyzed in details. As a result an excess of "radio quiet" C-class flares has been established for the near maximal flare active phase of Zurich cycle No 21 (1981–1983 AD). There is a general downward tendency in the relative parts of the stronger M and X class flares for the whole period of regular satellite X-ray observations since 1968 AD. The corresponding negative trends are nonlinear. Their absolute minimums has been reached during the rising phase of cycle No 23 (1997–2000 AD) and after that a "saturation" until 2014 AD is observed.
Key words: solar X-ray flares; solar radio emissions; sunspots; solar activity - indices; solar cycle

1. Introduction

Solar flares and coronal mass ejections (CMEs) are among the most energetic and spectacular solar activity events, which can release a vast amount of plasma and magnetic flux into the outer space and cause interplanetary disturbances and geomagnetic storms near the Earth (Gosling., 1993; Webb et al., 1994).

In practice, the solar flares emit in a wide range of wavelengths (from gamma to radio waves), which originate in different regions of the solar atmosphere. Many of the flares are the primary sources of radiobursts (e.g. Kim et al., 2009; Lobzin et al., 2010), as well as a significant increase of the solar electromagnetic radiation in the X-ray and EUV ranges (e.g. Sterling et al. 2000; Tripathi et al. 2004). There is strong association between the powerful solar X-ray (SXR) flare classes M and X, and the radiobursts in meter and decimeter range. A relatively small number of exceptions is associated mainly with the weaker C-class flares ("radio-quiet" flares) (Bentz et al., 2005). The strongest flares (e.g. SXR class X), often associated with interplanetary CMEs are related to the so called "Forbush-decreases" (FD), i.e. the temporary fading of galactic cosmic rays fluxes from 3 to 15–20% in comparison with their common levels. Such strong flares are also sources of solar energetic particles (SEP), such as protons, electrons or heavy ions with energies up to 1 GeV or higher (Reames, 2004). The SEP penetration into the middle and lower Earth's atmosphere is very high. There are few tens of cases when radiation enhancement events penetrated to the ground level between February 28th, 1942 and now (December, 2014) that were caused by SEP.

For these reasons, the strong solar flares and the associated with them CMEs, SEP-events, and geomagnetic storms are of high importance for many processes in the middle and low Earth's atmosphere. Moreover, these events play a crucial role for the stability and security of many components of the human technological infrastructure (communications, electric power grids, electronic equipments, radiative environments of the upper troposphere aviation, etc.).

Reliable predictions of the solar flare activity are an important task both from the scientific and applied points of view. Especially the predictions of the powerful X-ray flares of classes M and X need good algorithms. However, the correlation between strong solar flare classes and the sunspot activity (Schwabe- Wolf's cycles) on long time scales is relatively weak (see Table 1). Kiliç (2009) and Kane (2009) have pointed out that unlike the radio index $F10.7$, the differences between solar flares and sunspots behavior are very significant during the decreasing phase of the Zurich cycle 23. According to the analysis of (Kane, 2009), the last statement could be generalized for all corpuscular events in the solar atmosphere and interplanetary space. In this respect, it should be noted that a significant part of the most powerful solar flares of class X have occurred between 2003 AD and 2007 AD, during the fading solar cycle 23, i.e. during the moderate and the low sunspot activity conditions. For the purposes of predicting solar flare activity, one should build models based not only on the relationships between flares and sunspot activity, but also on other solar events, whose physical nature is more closely related to that of the flares. For example, such events could be the radiobursts of different types. These models cannot be used directly to make predictions, because they require information in advance for the levels of predictors, on which the flare activity depends. However they could help to detect some important dynamical features of the flares, such as trends and statistically important cycles. Achieving this goal requires as long as possible homogeneous data series.

In 1936 AD (Link and Kleczek, 1949), the epoch of relatively regular solar flare observations in the optical range began. But we note that some uncertainty concerning the data during the World War II exists. There is a homogeneous series since January 1976 that is published and regularly updated by the National Geophysical Data Center (Knoška and Petrásek, 1984; Ataç and Özgüç, 1998). The regular observations of the solar flares in the soft X-ray (SXR) spectral channel 1–8 Åby GOES satellite series, starting in September 1975 are available. Soft X-ray flares are classified according to the order of magnitude of the peak burst intensity measured in the 1–8 Å band, which are as follows: C-class ($10^{-6} \leq I < 10^{-5}\ W/m^2$), M-class ($10^{-5} \leq I < 10^{-4}\ W/m^2$), X-class ($I \geq 10^{-4}\ W/m^2$). There are also earlier data from the SOLRAD satellite from March 1968 up to February 1974, leaving an empty "window" without observations of approximately 1.5 years.

To the present day (December, 2014), the observational data of GOES SXR flares cover about 37 years. If the GOES data could be connected to the older one of the SOLRAD satellite, the total period of SXR flares data will cover 44 years. Such an extension could help with searching for temporal tendencies (cycles and trends) longer than one Schwabe-Wolf's cycle. This statement refers to the overall SXR flare events, as well as the separated strong flare classes C, M, and X, and their relative distributions during the four sequential solar cycles.

The main aim of this study is to build synthetic series for the monthly and yearly numbers of SXR solar flares of C, M, and X classes since January 1968. Unlike the first stages of our study (see Komitov et al., 2010) and taken into account the recommendations of other researchers, now the almost whole GOES satellites data set since January 1976 is used as input. In our early study the GOES data from the first four years between 1976 and 1979 AD has been not used for building of the models by doubts that they are not enough sensitive in the lowest power range and some of the C-class flares events probably has been not detected. On the basis of SXR flares data sets the multiple regression models for the monthly numbers of C, M, and X-classes flares are obtained. As factors (predictors) the monthly number of the radiobursts at three frequencies in the MHz and GHz ranges and the standard solar index $F10.7$ (radio flux at 2800 MHz) are used. There are two reasons for using radiobursts monthly numbers: 1) The relationships between the radiobursts and solar flares events (e.g. Shanmugaraju et al. 2003, Huang, Yan, and Liu, 2008), 2) In some stations the long-term radiobursts data sets have good coverage for the period since 1965–1967 AD. Thus, they could be used for successful reconstruction of the solar SXR flares since the beginning of the 1968 AD period on the basis of the obtained multiple models. In this work for comparison with the synthetic data from the corresponding periods, the earlier SOLRAD satellite data (before 1976 AD) are also used.

Finally, an essentially improvement of the C-class flares model and in a little degree for M-class model by using of time series analysis of residuals between the original and multiple models data has been reached. The corresponding procedure is described in Section 2.3.

2. Data and methods

2.1. The data

The solar flares are strong non-stationary processes of duration in range of minutes. Therefore they should be studied against not only the relatively smoothly changing indices, like the daily values of the International sunspot number Ri, or the radio-index $F10.7$, but also with other non-stationary phenomena, like the radiobursts in MHz and GHz spectral ranges. On the other hand, the flares influence the solar wind parameters and consequently the galactic cosmic ray (GCR) flux. Thus, the data for the GCR neutron fluxes (N_F), measured by the Moscow station is also used as a proxy for the solar wind, and its relationships with the flares of C, M, and X-classes is studied. The most part of the data necessary for this study, namely SXR flares (SOLRAD and GOES data), International sunspot numbers

Ri, solar radiobursts, $F10.7$ radio-index, and GCR (N_F), are published and regularly updated at the National Geophysical Data Center (NGDC) at $ftp://ftp.ngdc.noaa.gov/STP/SOLAR\_DATA$. The sunspot data are published in $http://solarscience.msfc.nasa.gov/greenwch$. The mean monthly data for the Longitude Asymmetry sunspot area index (LA) and "hemispheric" LA-index (Δ_{NS}) for the period 1964–1995 AD has been kindly given up by Prof. E. Vernova.

Our preliminary analysis in the published by NGDC radiobursts data shows that the most suitable ones in the whole data volume are the data from Sagamore Hill ($\varphi = +42$, $\lambda = -71$) for the frequencies $f = 606$–609, 8800, and 15400 MHz. First, they cover a wide frequency range, where the radiobursts are very often occuring. Second, these observations constitute a long and continuous in time series since the middle of 1960s (at least since 1967 AD). There are also other very qualitative data sets of the same, or similar frequencies from other stations, but only for more recent periods — since 1975–1980 AD, i.e. outside the interesting for us solar cycle (SC) No 20. We chose for the aims of our study the Sagamore Hill's data since January 1968 up to the end of 2009 AD. Thus, during this 42 year interval the near maximal and downward phase of SC 20 plus the whole next three solar cycles (SC 21, 22, and 23) are included.

Unlike to our previous study (Komitov et al., 2010) the data set from Upice (Czech Republic) at $f \approx 30$ MHz is not used. There are two reasons for that:

1. The continuous observations in Upice have been started since May 1972, i.e. the first four years of the studied period are not covered by these data. Thereby it is not possible to use these data for building of general regression models for the whole period, based on all four radiobursts data. In our previous study we use two types of models for reconstruction of flares including radioburst data at $f = 30$ MHz for the period 1973–2009 AD and without this frequency for the earliest time interval (1968–1972 AD).

2. In the multiple relationships for the all three classes of X-ray flares the effect of radiobursts at $f = 30$ MHz is clear detectable, but too small.

However, the radioburst data for $f = 29$ MHz, as well as for three other frequencies, monitored in Sagamore Hill (245, 1416, and 2695 MHz) has been used for some additional tests. For independent tests of our basic results the monthly numbers of sudden ionospheric disturbances (SID), detected in Upice and Panska Ves since the beginning of 1970th are used, too. As it is well known, the SIDs is lower ionosphere phenomena, which are strongly related to the solar X-ray solar flares. All these results are briefly discussed in Section 3.3.

The radioburst frequency 606–609 MHz is in interval. This is because during the period under investigation the observed frequency was changed to another situated very close to the first one. In this case, we assume that there are no significant differences and the observed radiobursts are related to the same phenomena.

We prefer to use in our study the monthly numbers of solar C, M, and X-class flares and radiobursts. They are easily comparable with the monthly values of the important solar indices like Ri and $F10.7$, which could be downloaded from the NGDC STP-server. The neutron GCR-fluxes are published as monthly data, too. This is important for the purposes of our study, which is focused on multiple regression analysis as a method. Other features of flares and radiobursts, for example, the stability of the corresponding active centers, are not a subject of this paper. That is why using another, “natural”, time step like the Carrington’s rotation period is not necessary. The data for SID-events are also based on STP server.

Another important problem, which could arise, is whether the radioburst data from only one isolated station (Sagamore Hill) are a good enough proxy of the solar radioburst activity for the chosen frequencies at all. This is due to the fact that the observations are provided only during the daytime. We assume in our study, that there is no significant radioburst activity difference between day and nighttime. Thus, the detected radioburst numbers, which we are using, are approximately half of the real ones if the whole daytime is used for observations. However, this assumption might not correspond well to reality for a number of reasons, for example seasonal effects.

That is why we decided to test this empirically by comparing the data from Sagamore Hill and Palehua stations for a sufficiently long period — 30 years (1980–2009 AD). The Palehua station ($\varphi = +21$, $\lambda = -158$) is the best situated of this purpose for three reasons: 1) Like Sagamore Hill, it is in the Northern hemisphere and thus, there should be no large seasonal effect differences with Sagamore Hill; 2) There are regular observations in Palehua during the above-mentioned period at $f = 606$–609, 8800, and 15400 MHz; 3) There is a large longitudinal and diurnal difference between these two stations ($\Delta = 87°$), i.e. the daytime begin and ended in Palehua almost 6 hours later than in Sagamore Hill. Palehua should observe large number of radioburst events, which are not observable from Sagamore Hill at the end. If there is no essential diurnal effect the corresponding monthly radioburst numbers based on both stations should be approximately equal.

We constructed linear regression of the form $N_{SGM} = aN_{PAL} + b$, where N_{SGM} and N_{PAL} are the monthly numbers of radiobursts observed from Sagamore Hill and Palehua at the corresponding frequences. As a result the following values for the parameters are obtained: $a = 1.23$, $b = 0.41$, and coefficient of correlation $r = +0.896$ for $f = 606$ MHz; $a = 1.14$, $b = 0.41$, and $r = +0.900$ for $f = 8800$ MHz; $a = 1.02$, $b = 0.76$, and $r = +0.874$ for $f = 15400$ MHz. The all three a coefficients are close to 1, while b coefficients are close to 0, i.e. it is approximately true that $N_{SGM} \approx N_{PAL}$. The slightly higher values of N_{SGM} vs N_{PAL} are very difficult to discuss, but most probably this is related to some differences in the technique and the local conditions of observations. The correlation between both station data sets is also tight enough ($r \approx 0.9$). These results demonstrate that the radioburst data from one separate station, if they are uninterrupted, is a good proxy for the radioburst activity of the Sun as a whole.

2.2. The multiple regression analysis (MRA)

For performing multiple regression analysis (MRA), many different algorithms are used. Here we take one of the most standard ones. As a first step, we need to determine the pairwise linear coefficients of correlation r between each pair of studied parameters. In our case they are: a) potential factors (predictors) – Ri, $F10.7$, N_F, N_{606}, N_{8800}, and N_{15400} (the last four are the monthly radioburst numbers at 606–609, 8800, and 15400 MHz); b) Predicted values: N_C, N_M, and N_X are the monthly numbers of C-, M-, and X-class flares. Thus, for every one of the predicted values, a series of one-factor minimized linear relationship with every one of predictors is determined.

On the basis of this preliminary pairwise correlation analysis one could select from all potential factors the essential ones. For this purpose we should consider not only the pairwise coefficients r between the potential predictors and every one of predicted values N_C, N_M, and N_X, but also the pairwise r between the each pair of predictors. An interesting and important case may arise when r between the two potential factors is high, i.e. the two are strongly related to each other.

An example for this one is the strong relationship between Ri and $F10.7$ ($r = +0.975$) (Table 1). On the other hand, both Ri and $F10.7$ are strongly correlated with N_C ($r = +0.847$ and $+0.856$, respectively). The closer relationship between N_C and $F10.7$ is easy to explain. $F10.7$ is more tightly connected with the parameters of the chromosphere and lower corona where the flares occur, while Ri is a photospheric index. Consequently, the relationship between Ri and N_C seems not to be independent and it is simply a consequence of the strong correlation between the "more appropriate" factor $F10.7$ and Ri. This comparison indicates that the independent relation between Ri and N_C, if it exists at all, is small. The same conclusions are valid for the parameter N_F, too.

Similar estimations were carried out for the two other indices N_M and N_X and their dependence on $F10.7$, N_F, and Ri. However, the final more exact estimations about the roles of Ri and N_F as factors can be obtained at the next stages of MRA.

The next step is building a series of multiple linear regression models of the type

$$Y = a_0 + \sum_{p=2}^{n} a_p X_p \tag{1}$$

where Y is the target index (N_C, N_M, or N_X) and X_p are the potential predictors. The procedure starts by building two factor models ($p = 2$) for each of the flare classes, after that three factor ones, etc. In our case the base factor is $F10.7$ (due to the best parewise correlation with the flare indices). We combine it in two-factor models consequently with Ri, N_F, etc. This is a critical moment for the whole procedure, because it helps in the final selection of the important and essential factors and removing from the additional analysis of those with a negligible independent effects over Y. The multiple coefficient of correlation R between the real and model data of Y and the Snedekor-Fisher's F-parameter are used as criteria. The Snedekor-Fisher's parameter is defined as $F = s^2_{tot}/s^2_0$, where s^2_{tot} and s^2_0 are the total and residual variances between the real and model data sets of Y. The relationship between F, R, and N (the number of observations) is

$$F = \frac{1}{1 - R^2}\frac{N - L}{N - 1} \tag{2}$$

L is the number of parameters in the regression model (for one-factor linear model it is 2, for two-factors linear one it is 3, etc.). In cases when $N \gg L$, like in this work, $F \approx 1/(1 - R^2)$. In practice $R \geq 0.65$, i.e $F \geq 1.67$ is necessary in order for the model to be useful for practical purposes. The increasing of F when a new factor is added to the model, is an indicator that there is some independent detectable influence of this factor over the predicted value. For our purposes here we suggest that adding an extra factor to the model is justified if F increases by at least 1%.

We find that R and F do not increase when Ri or N_F are added to $F10.7$ in two- or three-factor models, i.e. they should be rejected as significant independent factors for the monthly flare numbers N_C, N_M, and N_X. On the other hand, adding the radiobursts indices N_{606}, N_{8800}, and N_{15400} leads to a significant increase of the multiple model quality (see Section 3). In that case, it is necessary to take into account that the radiobursts at different frequencies are related to the physical conditions in the different layers of the solar atmosphere during the flares.

As a third step of our MRA algorithm we add to the best linear models for N_C, N_M, and N_X non-linear terms like X^2, X^3, X^4, $\exp(X)$, $1/X$, $1/X^2$, $\ln(X)$, $\sqrt{X}$, $1/\sqrt{X}$, as well as interactive terms of type X_1X_2 and X_1/X_2, where X_1 and X_2 are two potential factors. The procedure for estimating the importance of each non-linear term is similar to the procedure just described for each factor in the linear models and the criteria are substantial changes of R and F. But one should be very careful when using models containing strong non-linear terms ($X3$, $X4$, $exp(X)$, etc.) for extrapolations. The reason is that these models could be unstable outside the data set, on the basis of which they were obtained. To a less degree, this is valid for the pure linear models, too. A test for the model stability is necessary. Such one has been provided and described in our first study (Komitov et al., 2010).

It could use the obtained multiple models to extrapolate backwards in time the monthly numbers of C, M, and X flare classes and to create their "synthetic" data series since January 1968.

2.3. Time series analysis based on the T-R periodogramm procedure

As it is described in Section 3 the coefficients of multiple correlation R of the obtained best regression models for C, M, and X-flares are in the range of 0.77 to 0.9. They correspond to F in order of 2.5 to ~ 4 and residual variance in the range from 15 up to 40% from the total variance, i.e. there are significant deviations of model to real data in many cases. In the case when all important factors are included and no additional enough independent factors are known (it is our case) the last possible way to improve the models is to study for some inner regularities (for example cycles) in the "residual" series. The last ones are determined as deviations between the corresponding observed and modeled values.

We use for obtaining of statistically significant cycles in residual series the "T-R periodogramm procedure" (Komitov, 1997; Komitov and Kaftan, 2003; Bonev et al., 2004). According to this method the studied time series is approximated on the base of the least squares procedure by series of simple periodic functions of type:

$$\varphi(t,T) = a_0 + A\cos\left(\frac{2\pi t}{T}\right) + B\sin\left(\frac{2\pi t}{T}\right) \quad (3)$$

where T is the period, which increased by step ΔT from some initial chosen minimal value T_0 up to chosen maximal ones T_1, t is the corresponding time as a current number of values starting from 0 (i.e. $t = 0, 1, 2, \ldots, N-1$)) and a_0 is the mean value of the studied primary series terms. The local statistically significant peaks of coefficient of correlation $R(T)$ between $\varphi(t,T)$ and the primary series corresponds to statistically significant cycles by length of T in the last one. Some local peak is statistically significant by 95% probability if $R/\sigma_R \geq 2$, where σ_R is the error of R, i.e. $\sigma_R = (1-R^2)/\sqrt{N}$. Komitov (1997) suggests also a much stronger criteria when $R/\sigma_R \geq 3.5$ if $N \to \infty$. A comparison between T-R procedure and wavelet analysis has been made by Bonev et al (2004) and a very good agreement has been established.

On the basis of m established statistically significant cycles it could build a modeling function of the primary data series, which is described as:

$$Y(t) = a_0 + \sum_{j=1}^{m} \varphi(t, T_j) \quad (4)$$

The possibility to use $Y(t)$ for extrapolation (prediction) has been demonstrated due to "epignosis-test" by Komitov and Kaftan(2003).

We use the T-R procedure in this work for finding regularities (cycles) in residuals between the primary observed C, M, and X flares data series and corresponding multiple regression models of type (Eq. 1) and building models of type (Eq. 4). On this base new improved models are composed due to adding of models of type (Eq. 4) to the corresponding models of type (Eq. 1). We use these improved models for extrapolation before January 1976, i.e. since January 1968 and to obtain better "synthetic" series.

3. Results and analysis

3.1. The soft X-ray solar flares, sunspots, $F10.7$ index, cosmic rays, and radiobursts

The pairwise coefficients of linear correlation r between the monthly values of international sunspot numbers (Ri), solar radio flux at $\lambda = 10.7$ cm ($F10.7$), the neutron flux data from Moscow station (N_F), and the monthly numbers of solar flare classes C (N_C), M (N_M), and X (N_X) for the period 1976–2009 AD are listed in Table 1.

All coefficients of correlation listed in Table 1 are statistically significant. The negative values of r for the N_F data are as a result of the Forbush-effect, i.e. the reverse relationship between the GCR (N_F) and the overall

Table 1. Pairwise coefficients of linear correlation r between the monthly values of 6 solar and solar-modulated indices for the period January 1976 – December 2009

	Ri	$F10.7$	NF	N_C	N_M	N_X
Ri	1	0.975	-0.798	0.847	0.719	0.449
$F10.7$	0.975	1	-0.796	0.856	0.759	0.487
NF	-0.798	-0.796	1	-0.724	-0.615	-0.464
N_C	0.847	0.856	-0.724	1	0.672	0.415
N_M	0.719	0.759	-0.615	0.672	1	0.770
N_X	0.449	0.487	-0.464	0.415	0.770	1

solar activity level. Clearly, the N_C index (C-class flares) is significantly more tightly related to the Ri and $F10.7$ than the N_M and N_X indices of the stronger M and X flares.

The correlations of the N_M and N_X indices with Ri and $F10.7$ are significantly lower, but like N_C their relation to $F10.7$ is also stronger than the one to Ri (Table 1). An interesting feature is the weak correlation $(0.4 < |r| < 0.5)$ of the X-class flares (N_X) to almost all other indices in Table 1, except that of the M-class flares (N_M), for which $r = +0.76$. Such low values of r could be explained by the specifics of the X-class definition (see Section 1). The criterion for classifying a SXR flare to X-class is that its intensity exceeds $10^{-4}\ W/m^2$. There is no upper limit for X-class flares, unlike the flare classes C and M. So, to the X-class could be comprised of events with very different energy characteristics, which probably occurred in very different physical conditions in the solar atmosphere. High variance within the X-flare class is the reason for the low r values listed in Table 1.

It has been already mentioned in Section 2.2, that the high value of r between Ri and monthly flare numbers is rather due to the very tight relationship between Ri and $F10.7$. Recently, it has been finally confirmed by the MRA procedure, that the important factor for the all three flare indices N_C, N_M, and N_X is $F10.7$ (Fig. 1) and there is no any significant independent influence of Ri.

The radioburst monthly numbers (Fig. 2) are not closely related to the overall solar activity indices such as $F10.7$ (Table 2). Because the correlation coefficients of the three selected radioburst frequencies span the range 0.52–0.62 (Table 2), they could be taken as sufficiently independent factors in the multiple regression models.

Table 2. Pairwise coefficients of linear correlation between the monthly radio bursts numbers and $F10.7$ index.

	$F10.7$	N_{606}	N_{8800}	N_{15400}
$F107$	1	0.619	0.586	0.524
N_{606}	0.619	1	0.905	0.884
N_{8800}	0.586	0.586	1	0.961
N_{15400}	0.524	0.524	0.961	1

As it is shown in Table 2, the correlation coefficients between the monthly numbers of radiobursts at $f = 606$, 8800, and 15400 MHz are high ($r \geq 0.88$), i.e. they are quite closely related to each other, but not nearly as much as Ri and $F107$. The reason for using all three selected radioburst types is that including them simultaneously in our multiple regression models slightly improves them and, on the other hand, the Snedecor-Fisher's F-parameter increases between 2% and 5% for each one added radio frequency for N_C. For N_M and N_X this improvement is much higher.

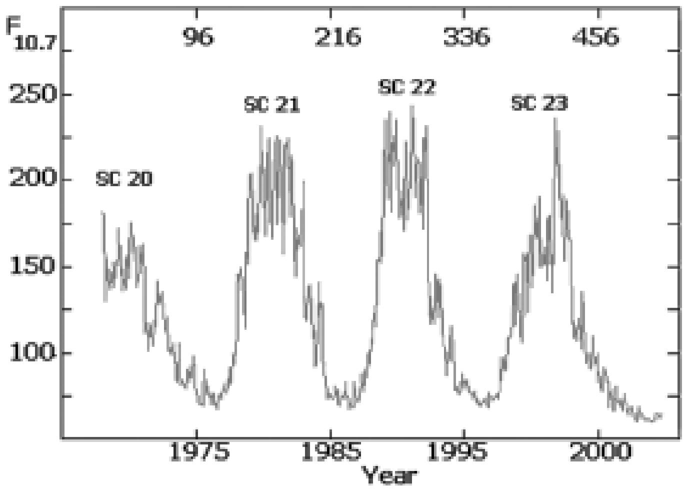

Fig. 1. The mean monthly $F107$ series (January 1968 – December 2009).

3.2. The SXR flares (1976–2009 AD): multiple regression models

After a lot of statistical experiments we found that for the epoch January 1976 – December 2009 the following multiple minimized functions are the best approximations for the considered C, M, and X classes of SXR solar flares.

a) C-class flares:

$$N_C = -217.25 - 0.873N_{606} + 0.313N_{8800} + 1.552N_{15400} + 3.738F10.7 - 0.0084F10.7^2 \quad (5)$$

$R = 0.864$; $F = 3.89$

b) M-class flares:

$$N_M = 15.49 - 0.096.N_{606} + 0.498.N_{8800} + 0.456.N_{15400} - 0.333F_{10.7} + 0.0018.F_{10.7}^2 \quad (6)$$

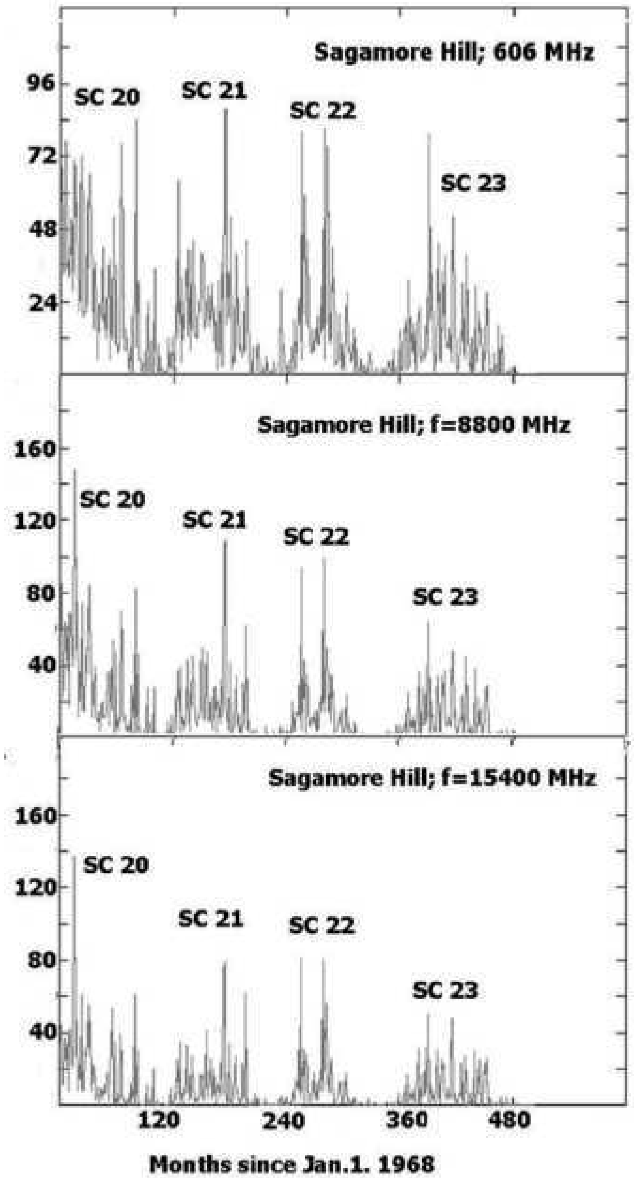

Fig. 2. The monthly radioburst numbers at f = 606–609, 8800, and 15400 MHz (January 1968 – December 2009).

$R = 0.920$; $F = 6.41$

c) X-class flares:

$$N_X = 2.1 + 0.0139.N_{606} + 0.0169.N_{8800} + 0.122.N_{15400} - \\ 0.0386F_{10.7} + 0.000164.F_{10.7}^2 \quad (7)$$

$R = 0.788$; $F = 2.61$

The negative linear terms for the $F10.7$ index in both Eq. 6 and Eq. 7 indicate anticorrelation of the radio flux with the M- and X-class flares at low and medium levels of this index. The relationship changes to positive when $F10.7 > 185$ for the M-class or $F10.7 > 235$ for X-class flares. The C-class monthly numbers increase slowly at higher levels of $F10.7$, which is marked by the negative sign of the quadratic term in Eq. 5. One could conclude that the increase of the M- and X-class flare activity is most probably due to the reduction of the C-class events. Furthermore, such reducing of the C-class flare activity could probably lead to the shifting of the mean energy of flare activity from lower to higher energetic classes. Thus, it could explain also why the critical "threshold" for X-class flares ($F10.7 = 235$) is higher than M-class flares ($F10.7 = 185$). The both values are slightly lower than in our first study, where they are 210 for M and 245 for X-class, correspondingly.

It is interesting to compare the models (Eq. 5 – Eq. 7) with the "pure" $F10.7$-models for the flare monthly numbers N_C, N_M, and N_X, i.e. if the radiobursts are fully excluded as factors. We have investigated relationships of the form $N_V = a.F10.7^2 + b.F10.7 + c$ (V is C, M, or X). In this case the corresponding R and F values decrease and $R = 0.854$ and $F = 3.68$ for N_C, $R = 0.782$ and $F = 2.56$ for N_M, and $R = 0.512$ and $F = 1.35$ for N_X. These results demonstrate that including the radiobursts plays **have** a significant role for the C-class flare models and is very important for the models of M-class, and especially of X-class flares.

Equations 5–7 were obtained on the basis of GOES data from 34 years (1976–2009 AD). We can consider them as the most representative and accurate for the flare classes C, M, and X. They could be used for the whole period of their extrapolation (1968–1975 AD, i.e. for the whole period of SOLRAD observations (March 1968 - February 1974) plus an "empty" interval of 18 months (March 1974 – August 1975) without observations. But before that we decide to make some additional analysis of the satellite data, as well as to improve the models Eq. 5 – Eq. 7.

The observed monthly numbers of C, M, and X-class flares (SOLRAD + GOES satellite observations, 1968–2009 AD) are plotted in Fig. 3. By our opinion, there is an evidence that the early C-class instrumental data is indeed lower than the actual numbers of such flares is shown in Fig. 3 (top panel). A systematic shifting up of the whole plot since ∼1976 AD (i.e the start of GOES observations) relative to the earlier epoch is clearly visible. In our opinion, this is rather clear indication for existing of significant instrumental effect. Such effect is not detectable in the plots of N_M and N_X (Fig. 3, middle and bottom pannels), as well as in the radioburst plots in Fig. 2.

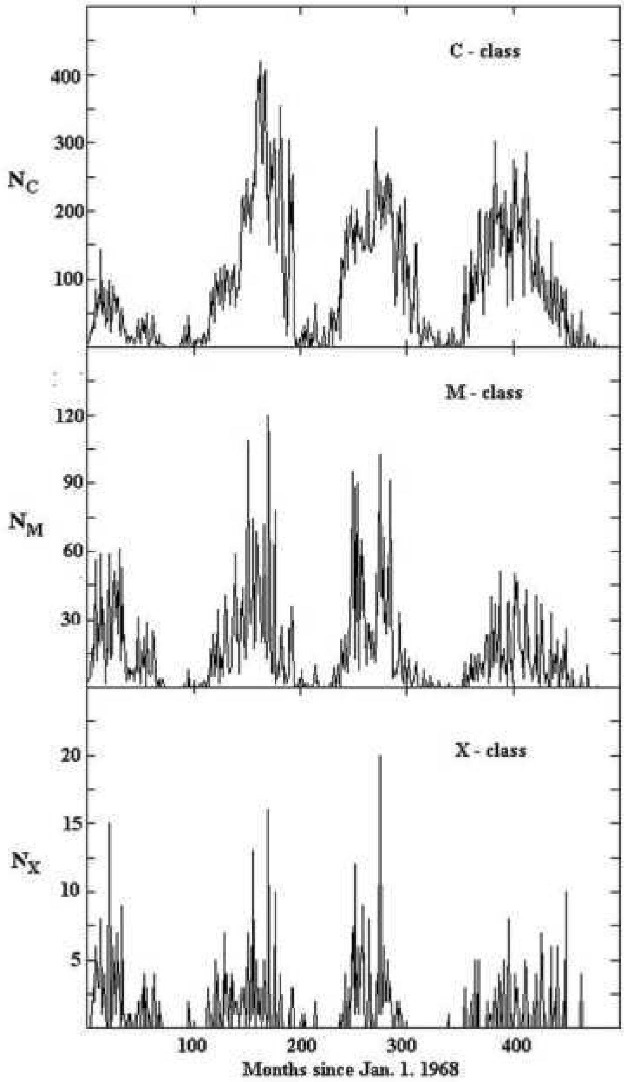

Fig. 3. The observed satellite SXR flares monthly numbers (March 1968 – December 2009 AD). The plotted data are as follows: a) from SOLRAD — between the months 1–72 (March 1968 – February 1974 AD); from GOES 1–14 — since the month 92 (August 1975 AD). There are not instrumental data between the months 73–94 (March 1974 – August 1975 AD).

3.3. Searching for additional factors

As it has been already pointed out in the course of the present analysis a large number of multiple regression models has been tested. We tried to improve the last ones by including of radioburst monthly numbers for additional frequencies with enough long and continuous time series, i.e. covering the whole period 1968–2009 AD. Only few other time series are responding of these requirements — the radiobursts data sets from Sagamore Hill at 245, 1415, 2695, and 4995 MHz. They has been used as additional predictors in our models, including a building up to 8-factor regression models (606, 8800, 15400 + 245, 1415, 2695, and 4995 MHz + $F107$ index). It has been found that such adding does not lead to essential improvement of the models, i.e. the corresponding R and F parameters tend to "saturation" when three or four radiobursts frequencies in the range 200–20000 MHz are used. As it has been already noted, some detectable improvement occurs when the $\sim$30 MHz data set from Upice is added, but the corresponding radiobursts time series begin since May 1972 AD.

It has been also tried to improve the MRA-models by including of many other solar and geophysical indexes, which could be by our opinion eventually good proxies of solar flares — such as sudden ionospheric disturbances (SID), the north-south sunspot area asymmetry, the longitude asymmetry sunspot area index (LA) (Vernova et al., 2002) and the "hemispheric" LA-index (Δ_{NS}) (Vernova et al., 2002). Unfortunately all these tries has been non-successful, too.

3.4. Analysis of "residuals"

It is obviously that independently of the essential advances of multiple correlation relationships, including factors $F10.7$-index and the three radiobursts monthly numbers in relation to one-factor relationships, the residual variation of models (Eq. 5 – Eq. 7) remains too high. It is about 25% (Eq. 5), 16% (Eq. 6), and 38% (Eq. 7) from the total variance for C-, M-, and X-class flares, correspondingly. That is why in this subsection, analysis of the "residuals" ("real-model" data values) for the whole GOES data set period (1975–2009 AD) is made. It could help by study of the features of these residuals to be made some conclusions and hypothesis about other possible factors, which has been not taken into account in models (Eq. 5 – Eq. 7). As it has been already noted in Section 2.3, it is interesting in this course to search for some regularities (it meant mainly cycles) in the "residual" series by using of T-R method. The next step should be the build on the basis of obtained cycles dynamical models of residuals and add it to the "basic" one: regression models ((Eq. 5 – Eq. 7)) as it is described in Section 2.3. The next step in this sequence is to extrapolate the "combine" model to the past, namely for the period 1968–1975 AD. Finally, we build the "synthetic" series, i.e. the calculated monthly numbers of C, M, and X flares for the period January 1968 – August 1975 plus the original GOES data for the recent period (August 1975 – December 2009). An additional task is the comparison between the model data for the period of March 1968 – February 1974 and the corresponding measurements of SOLRAD satellite during the same period. On this base it could made additional estimation for confirmation or rejecting the conclusion about higher real levels of C-class flare activity during the Zurich cycle No 20 comparing to the corresponding SOLRAD satellite instrumental data.

The residuals between the original GOES data during the "basic" period (1976–2009 AD) for the C-, M-, and X-class SXR flares and the corresponding modelling values, calculated by regression Equations 5–7 are plotted on Fig. 4. The following features are shown:

1. The time distribution of residuals seems strong non-randomized. The negative values are predominantly placed during the rising and near-maximal phases of the last three Schwabe-Wolf's cycles (SC 21, 22, and 23), i.e. there are less real flares as it is follows by the corresponding regression models.

2. The higher positive deviations are predominantly 1-2 year after the sunspot maxima of corresponding cycles. They are higher for SC 21 and 22 and smaller for SC23. The effect is less expressed for M and stronger for C and X class flares.

3. The models (Eq. 5 – Eq. 7) are in better conformation with the "moderate high" Zurich cycle No 23 as with the higher SC 21 and 22.

The high regularity of residuals is a clear indication that there is some another significant factor, which is not included in model (Eq. 5 – Eq. 7). As it is shown in the residuals, the last one is connected to the macroparameters of corresponding sunspot cycles like their phase, magnitude, length, etc. What are these factors, why their influence over flares could not be included in $F10.7$ or Ri ones it not still clear.

A possible explanation for the excess of high positive deviations during flare maximum of SC 21 in 1981–1982 could be the large number of weakest C-class flares in magnitude range (C1–C5). As it has been pointed by Benz et al. (2007) the SXR flares with magnitude less than C5 are predominantly "radio-quiet". They are not associated to radioburst events. Indeed, this is the case, which is observed for SC 21 flare maximum. We have test this hypothesis by an additional extracting only of the month numbers of flares in magnitude range C1–C5. It has been found that really close after the main sunspot maximum in 1979–1980 an excess of large number "weak" C-class flares exists during 1981–1983.

3.5. T-R periodogramm analysis, combined models and "synthetic" series

We have studied the "residual" series plotted in Fig. 4 (the period 1976–2009) for statistical significant cycles by using of T-R procedure. In all separated procedures for C, M, and X-class flares the initial period is chosen as $T_0 = 2$, the maximal period is $T_1 = 360$, and the scan step ΔT is 0.5 months. On the basis of the cycles with highest statistical significance, for which $R/\sigma_R > 3.5$, the dynamic models $Y(t)$ (see Section 2.3) for the residuals of C, M, and X class flares are build. The lengths of most important obtained cycles are as follows :

- for C-class: 55.5, 69.5, 106.5, 131.5, and 228 months;
- for M-class: 44, 67, 70, and 90 months;
- for X -class: 21, 63.5, 91, 129.5–134, and ~225 months.

It is obviously by these results that there are cycles, which are close to the sunspots Schwabe-Wolf's cycle length (~ 133 months or 11.1 years), as well as a cycle by duration relatively close to 22 yr Hale solar cycle (~

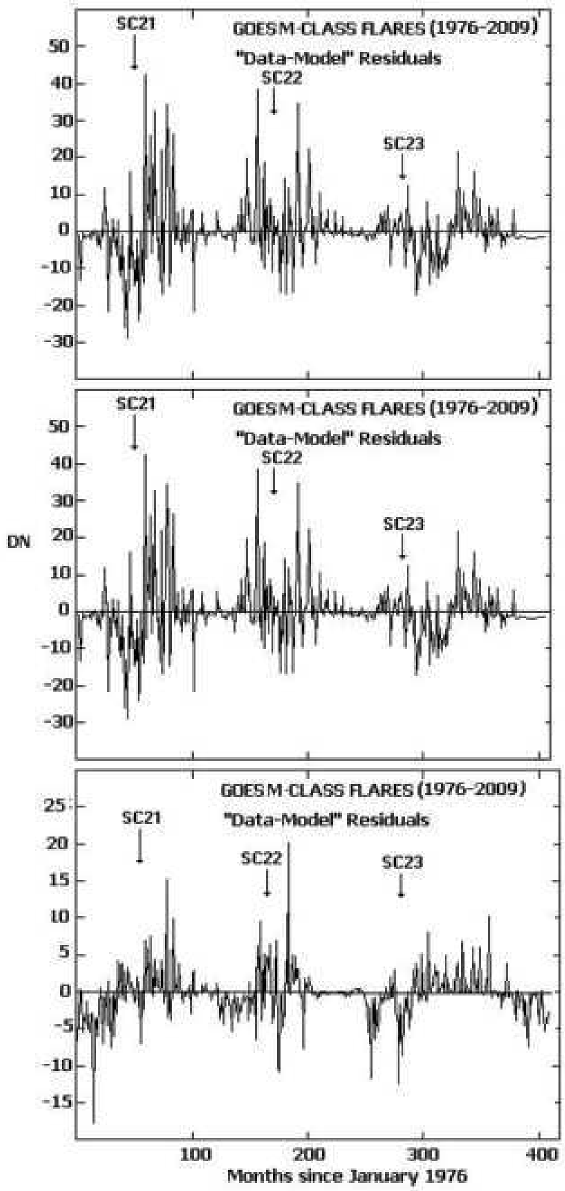

Fig. 4. The “Data-Model” residuals (August 1975 – December 2009 AD).

220–230 months or ∼19 years). There are also oscillations in the range 60–70 months, i.e. 5–6 years. Cycles with such duration (1/2 of 11 yr cycle) are often exists in some solar and geomagnetic indexes. Consequently the cyclic behavior of “residuals” is enough strongly connected to the overall solar activity variation and solar dynamo regime and they are in generally not occasional. May be it could be interesting to analyze and discuss these results in much more details, but it is not a subject of the study.

The multi-cyclic residual model functions $Y(t)$ on Fig. 5 are plotted. Extrapolations in the past (since January 1968) and in the future (up to December 2015) are shown, too. The multi-cyclic expression is much stronger valid for C-flares "residuals" series (upper panel) as for M and X flares ones (mid and bottom panels). The coefficient of correlation between $Y(t)$ and corresponding residual series for C-flares for the "referent" period 1976–2009 AD is about 0.57, which is essentially higher than the corresponding values for M and X-flares (0.35 and 0.45, respectively).

We add the $Y(t)$ functions for C, M, and X flares "residuals" to the corresponding multiple models (Eq. 5 – Eq. 7). There is an essential improvement for the composite model for C-class flares for the referent period 1976–2009 AD. The multiple coefficient of correlation increases from 0.864 to 0.916 when the obtained multi-cyclic $Y(t)$ for C-flares residuals is added to Eq. 5. The corresponding F-parameter increases from 3.89 to 6.20, i.e. the "non-explained" variance decrease from 25% to 16% from the total variance. The improvement of M-class multi-factor model (Eq. 6) by adding of corresponding $Y(t)$, plotted in the mid panel of Fig. 5 is essentially smaller — the relative part of "non-explained" variance decreases from 14% to 12%. There is no improvement for the X-class flares, when a composite model from multiple regression model (Eq. 7) and corresponding $Y(t)$ function is build. This fact could easy to explain: The poly-cyclic function $Y(t)$ is too flat and it not well correspond to the very strong discrete time series, such as this of monthly X-flare numbers. So for X-flares the most valid remains the multi regression equation (Eq. 7) without combination with "poly-cyclic" term $Y(t)$.

As it was already pointed the nature of founded cycles as well as the build $Y(t)$ functions is unknown on this stage. It is only clear that they are related to the overall solar activity regime. Although some additional features of $Y(t)$ are visible on Fig. 5. A general weak tendency "higher solar cycle amplitude → higher Y(t) amplitude" for C-flares series is shown. It could also track it in the both extrapolated parts — in future (SC 24) and in past (SC 20). On the other hand the weakest $Y(t)$ variations are shown for M-flares during the near maximal phase of SC 20, while for SC 24 the extrapolation procedure point an increasing of the $Y(t)$ for M-flares since 2009, local minimum near the maximal phase in 2012–2013 and increasing after that up to 2015 AD. It is important for the practical aims of our study that the bring of $Y(t)$ terms to the monthly C and M flares dynamics during SC 20 is relatively small and it shouldn't to expect any essential differences in their calculated values by using of the pure multiple regression models (Eq. 5 and Eq. 6) in relation to the case if an additional correction with the $Y(t)$ terms is made. In spite of that, we use $Y(t)$ corrections for C and M flares during the period 1968–1975) for a slight better precision.

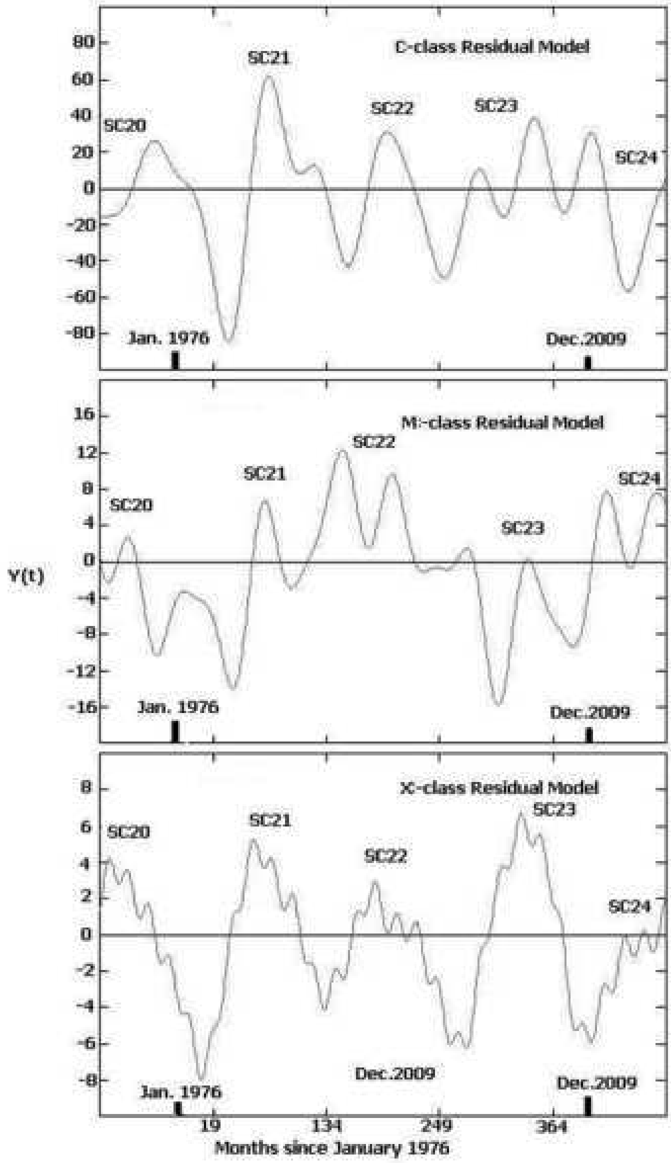

Fig. 5. The "poly-cyclic" $Y(t)$-model for C, M, and X flares residual series on the base of GOES satellite observations (1976–2009 AD) and its extrapolations for SC 20 and SC 24.

3.6. "Synthetic" solar flares series (January 1968 – December 2009 AD)

By using of "composite" models for C- and M-class flares, based on Eq. 5 and Eq. 6, and corresponding "residual" $Y(t)$-functions, as well as Eq. 7

for the X-class flares the modeled series for the period January 1968 – August 1975 has been calculated. The monthly numbers of the three class flares directly observed by GOES satellites for the period September 1975 – December 2009 are added to the calculated earlier parts of series. The so build "synthetic" series on Fig. 6 are shown.

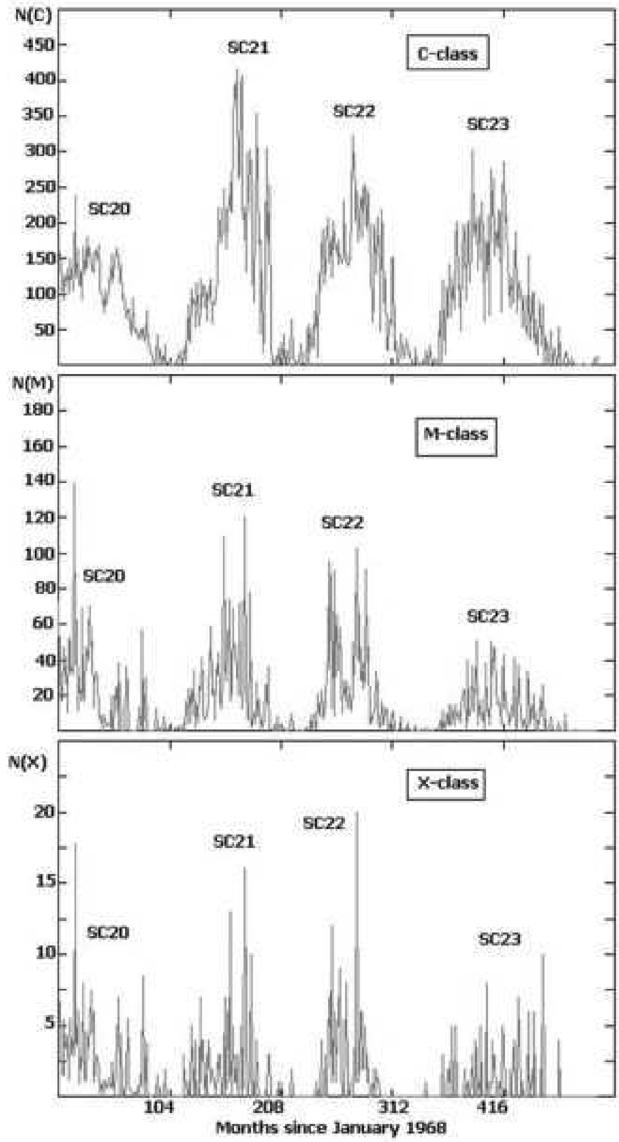

Fig. 6. The "synthetic" SXR flares time series for the period (1968-2009 AD).

The main differences between the original observed data sets (SOLRAD + GOES) and the "synthetic" ones concern the C-flares monthly numbers during the period of SOLRAD observations. The mean value of monthly C-class flare numbers for the period March 1968 – February 1974, calculated on the base of direct SOLRAD observations is 33.8 vs 117.6 by the modeling data. The corresponding values for M-class are 17.4 vs 22.5, while for X-class they are 1.8 vs 2.5. So, for the stronger classes M and X the ratio is in range 0.77 and 0.72, respectively, while for C-class it is only 0.29. As it was already noted above, the effect of $Y(t)$-terms during SC 20 are small for C- and M-classes. If they are not taken into account or, by other words if we use the "pure" (Eq. 5 and Eq. 6) the corresponding calculated ratios should be 0.68 and 0.30, i.e the ratio for M-class decreases slightly, while for C-class it is almost the same. Obviously the difference between the pre-calculated to "GOES-standard" and original SOLRAD data for M- and X-class flares during SC 20 is not so large (25-30%), while it is very serious for the C-class flares and the observed number of these events is 3–3.3 times smaller as it follows from the model.

Another evidence for a generally lower SOLRAD C-class numbers is shown on Fig. 7. The residuals between the original observed by SOLRAD monthly C-class flares and the corresponding composite model data on Fig. 5 (the top panel) are systematically negative. Moreover, the difference is almost constant (DN $\sim$ 100) during the near maximal and middle phase of SC 20 ($\sim$ 1968–1972 AD, the first 55–60 months). As it is shown on the middle and bottom panel on the same figure, the residuals for M and X flares are essentially smaller and there are negative as well as positive residuals between the SOLRAD and modeling data. It need note especially the good agreement between the observations and model for the M-flares.

On the base of these results it should conclude that:

1. There is an other evidence that in the SOLRAD data the C-class flare events number is underestimated in respect to the GOES 1–14 satellites data set (1976–2009). Most probably it is caused by significant instrumental differences of the SOLRAD measurements to the GOES ones, which reflects over the weakest C-class flares data. Thus, the real SC 20 C-class flare activity should be estimated as higher as the observed one.

2. The M- and X-class flare numbers in the original SOLRAD data correspond well to the models. Consequently, there are no significant differences between the GOES and SOLRAD observations in power magnitude ranges M and X and no re-estimation of SOLRAD data set needs for these classes.

3. It needs especially noted that the correspondence between the SOLRAD data and the pure MRA-models (Eq. 6 and Eq. 7) for M- and X-classes in their extrapolated part (1968–1974 AD) is even better as for the "basic" period (1976–2009 AD). It is evidence that the derived regression models in their present type much better describe the flare activity in rather moderate cycles as SC 20 and 23, as well as in the extremely high ones SC 21 and 22.

4. The adding of corrections on the base of $Y(t)$-terms helps for the better description of C, M, and X flares dynamics during the powerful cycles 21, 22, and 23. Their using gives a better quantitative expression of C and M flares during the same cycles. But on the other hand, the effects

of $Y(t)$-terms are small during SC 20. There is no significant difference if these terms are taken into account in modeling for SC 20 or the calculations only on the base of the "pure" MRA-models are made.

The calculated on the basis of the models yearly synthetic numbers of C-, M-, and X- class flares for 1968–1975 AD, plus the corresponding observed SOLRAD values are shown in A. The calculated monthly and yearly numbers of SXR flares on the basis of GOES observations during the period are shown in B, C, and D.

4. Discussion

In our opinion, the proposed in this study synthetic time series of the monthly numbers of SXR flares of C-class is more realistic in their earlier (modeled) parts (before 1976 AD) than the direct instrumental data from SOLRAD satellite observations. There is no significant difference between observed SOLRAD satellite data and modeled data for the M- and X-class flares during the period 1968–1974 AD. However, the models (Eq. 5 – Eq. 7) help us to have synthetic data for the period March 1974 – August 1975 where the SOLRAD observations have been already ended, but GOES ones have been not still started. Our time series models for the epoch 1968–1975 AD are based on multiple regression models with high statistical significance. The data for $F10.7$ and the monthly numbers of radiobursts at four frequencies for the period 1976–2009 AD are used as input parameters.

On the basis of this one for the same period of time we use GOES satellite SXR flares data with two assumptions: 1) These data are more qualitative and certain than the earlier one, before 1976 AD; 2) There are no significant physical causes for less validity of the obtained regression models during the earlier epochs.

It follows by our analysis that the $F10.7$ and radiobursts numbers are the best proxies for SXR flares multiple models. Other phenomena like SID-events, which are taken also as a good indicators for SXR solar flares are not too suitable. The same one is valid for many other not so "conventional" indices like LA, Δ_{NS} (Vernova et al. 2002; 2004), etc. But on the other hand, in the models (Eq. 5 – Eq. 7) the residual variance remain too high. Some reasons for this one has been discussed in Section 3.5.

As an "working" solution of the problem for the residual variance in this study we use a time-series analysis (the T-R procedure). The argument for such decision contains in the visible quasi-periodic regularities in the series of "residuals" (Fig. 4). It has been found that there are statistically significant oscillations by duration of 5–6, 11, and ∼20 years. On this stage it could only say that, most probably, the corresponding unknown factor (or factors) is connected to the overall solar solar activity variations regime. On the other hand, this factor (or factors) is not directly related to such "conventional" indices like $F10.7$, which is included in MRA-models (Eq. 5 – Eq. 7) or Ri. The analysis of $Y(t)$-terms , describing the overall quasi-cyclic behavior of the residual variance of MRA indicates that their effects are important for the higher cycles SC 21 and SC 22 and in smaller degree for SC 23. It is very small or almost negligible for the weaker cycles such as SC 20 and may be for SC 24, too. This conclusion is much more

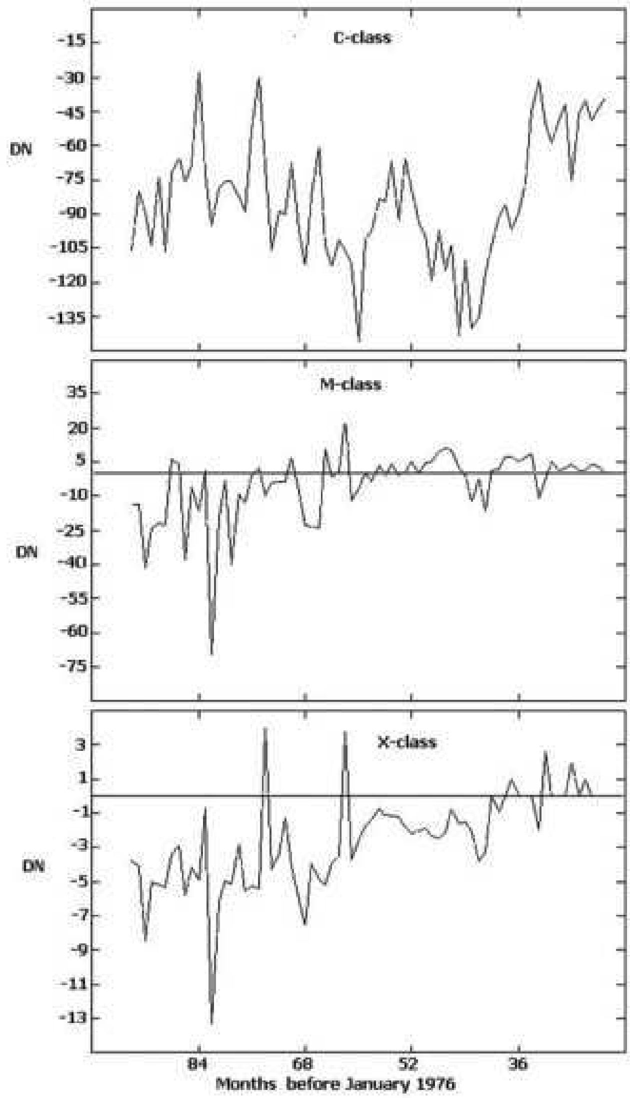

Fig. 7. The residuals "SOLRAD data – model" for the period March 1968 – February 1974 AD.

valid for the weak C-class flares as for M and X ones. The corresponding "poly-cyclic" $Y(t)$-function describes about 40% from residual variance of model (Eq. 5) during the period of GOES 1–14 observations (1975–2009 AD). Independently from all, the using of "poly-cyclic" approximations, based on time series analysis, solve the problem for the residual variance only particulary — a significant part of it remains out of description and explanation.

Consequently, a future improvement of the models, based on MRA is necessary. In some degree the present results, based on time series analysis, are good starting point for this one. However, there is a significant result, which has been established. The C-class flare activity during the near maximal and downward phase of Zurich cycle No 20 is greater as it follows by the published in STP-server SOLRAD data. Moreover, another very interesting phenomena could be also detected there. It is described below.

As it is shown in Fig. 6, the Zurich SC 20, which is the weakest in sunspot activity from the last four ones (SC 20–23) is comparable by SXR M- and X-class flare activity to the last three cycles (SC 21–23). It is shown in Fig. 2, that the near maximal and downward phases of SC 20 are too rich in radioburst events and it is a serious reason for this suggestion. The downward phase of SC 20 is very rich of M and X flares ?ven in the final pre-minimal phase before the start of SC 21 (Fig. 6). In contrary, there is total absence of M- and X-class flares during the next epochs of the sunspot minima in 1986, 1996, and 2007–2009 AD. Every one of these free of M and X flares time windows is wider than the previous one. A low activity of C-class flares is shown in 1986 and 1996 AD, and during the last deep minimum between SC 23 and 24 it is very close to zero. Fig. 6 show that SC 23 is significantly poorer of M- and X-class flares than the previous three cycles. The maximum of the X-class flare activity during this cycle is strongly delayed (3–4 years) in relation to the sunspot maximum. This delay is mainly due to the relatively high X-class flare activity in the period of the Halloween storms (October–November 2003) and the next 3 years before the deep solar minimum between SC 23 and 24.

All these facts suggest the existence of a well expressed downward trend from sunspot SC 20 to SC 23 for the activity of strong SXR flares of classes M and X, and the extreme (minimum) phase is reached near to or a little before the maximum of SC 23. To elucidate this effect, we use the smoothed 11 years (132 month) values of SXR flare numbers N_C, N_M, and N_X to calculate the ratios $f_M = N_M/N_{tot}$ and $f_X = N_X/N_{tot}$, where $N_{tot} = N_C + N_M + N_X$. We took f_M and f_X equal to zero in all cases when $N_{tot} = 0$. Thus, f_M and f_X present the relative parts (frequencies) of M and X class flares in the overall flare activity (C+M+X flares) for the corresponding time. The smoothed over 11 years values of f_M and f_X are shown in percent in Fig. 8.

During SC 20 the relative fraction of M- and X-class flares is higher than during the next three sunspot cycles. A clear downward tendency is shown for the relative presence of the both M- and X-class flares since the maximum of SC 20. It seems that this tendency reaches its deepest point in the second half of the 1990s, near 1998 AD. The high M- and X-class flare activity during 2003–2006 AD is obviously the main factor that stops this downward trend. Unfortunately, our synthetic time series are too short to allow us to make some more concrete assumptions and predictions for the M and X classes flare activity in the near future and especially for SC 24. It is very possible that the negative trend in the behavior of the relative parts M- and X-class flares (Fig. 8) is just a decreasing phase of a cycle with

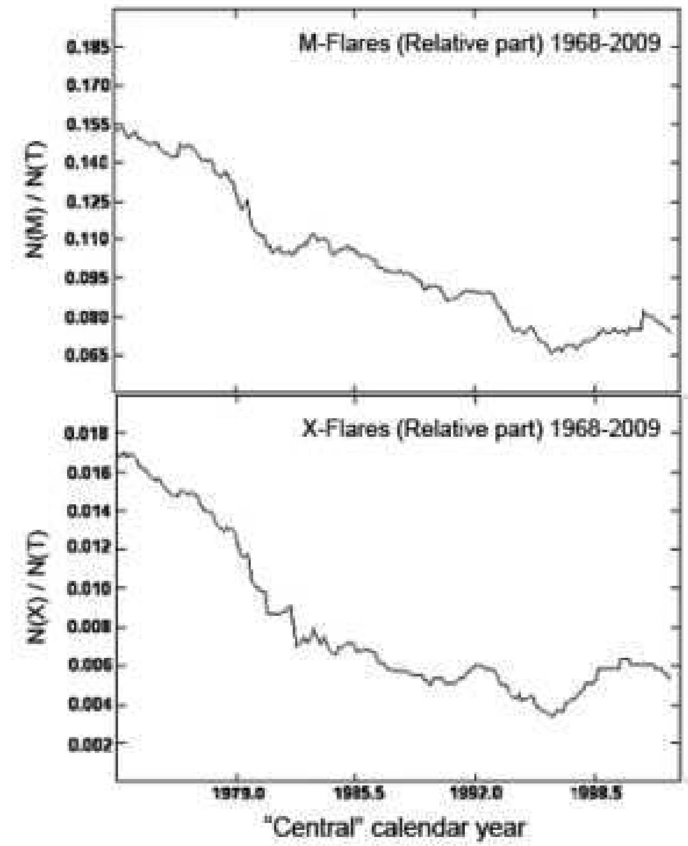

Fig. 8. The relative parts of M- and X-class flares during the period 1968–2009 AD.

sub-century or quasi-century duration. If it is so, an increase in the relative frequencies of the strong flares of M- and X-classes could occur even during the obviously low in sunspots SC 24. However, it is still difficult to take or reject this assumption at this stage.

We would like to point out that the conclusion about the downward trends of f_M and f_X remains even more valid on the basis of the original SOLRAD data before 1975 AD. The reason for this is the fact that the level of C-class flare activity according these instrumental data is lower than the synthetic ones, while the M- and X-class activity levels are approximately the same. This rapidly "drags up" of the f_M and f_X levels before 1975–1976 AD leads to a more pronounced downward trend.

During the final preparation of this paper a new study concerning the intercalibration between the data of different satellites (GOES and SOLRAD) has been published (Neupert, 2011). Our preliminary analysis of the main results in this study point out, that they could not affect very significant over our general conclusions even if they are taken into account.

5. Conclusions

The main results obtained in this study could be summarized as follows:

1. On the basis of the GOES satellite instrumental data for the solar SXR flares during the period 1976–2009 AD multiple regression models for the monthly numbers of C-, M-, and X-class flares were built. In these models the mean monthly radio index $F10.7$ and the monthly numbers of radioburst at the frequencies ∼606 MHz, 8800 MHz, and 15400 MHz are used as input parameters. The models are characterized by coefficients of multiple correlations in the range 0.78–0.92. The corresponding residual variance of these models is in the range of 25% (for class C), 16% (for class M) to 38% (for class X). By using of corrections based on time series analysis for C and M flares the residual variance of models for these two classes has been reduced to 16% and 14%, respectively.

2. Using these models, synthetic time series of the monthly numbers of C, M, and X class SXR flares were built for the period 1968–2009 AD.

3. Evidences for existence of a general downward trend of the SXR flare activity during the last decades of the 20th century was found. The trend is very well expressed in the smoothed relative frequencies of the strong flare classes M and X. Moreover, this negative trend reached its deepest minimum during the increasing phase of SC 23.

4. Most probably the rate of C-class SXR flare activity before 1975 AD has been underestimated during the earlier satellite observations with SOLRAD.

Acknowledgements

The authors thank the anonymous referee for the helpful suggestions and comments. The authors gratefully acknowledge the support of National Geophysical Data Center, Boulder, Colorado, U.S.A. for proving the data of SXR flares (SOLRAD and GOES data), International sunspot numbers, solar radiobursts, $F10.7$ radio-index, and GCR neutron flux via ftp://ftp.ngdc.noaa.gov/STP. The authors are also grateful to Dr. Jiri Simunek from Panska Ves Observatory for useful information concerning the SID-events observations, as well as to Prof. E. Vernova for the mean monthly LA and Δ_{NS} data.

A Yearly numbers of SXR flares of C, M, and X Classes (1968-1975 AD) (*rm* – synthetic data, *obs* – instrumental SOLRAD data)

Year	N(C)rm(A)	N(C)obs	N(M)rm	N(M)obs	N(X)rm	N(X)obs
1968	1505	***	450	***	49	***
1969	1629	775	516	323	56	40
1970	1810	676	475	416	45	38
1971	1295	165	89	99	10	5
1972	1625	287	141	159	25	17
1973	824	172	59	83	12	9
1974	556	***	119	***	19	***
1975	139	***	13	***	3	***

B Monthly and yearly numbers of C-class flares 1976-2009 AD (GOES 1-14 instrumental data)

Year	Jan	Feb	Mar	Apr	May	Jun	Jul	Aug	Sep	Oct	Nov	Dec	C-Total
1976	11	1	34	19	1	1	0	13	7	36	7	17	147
1977	18	32	33	38	24	75	27	36	77	65	56	132	613
1978	89	203	175	173	243	175	150	112	225	196	165	195	2101
1979	221	252	209	231	219	220	200	237	236	230	218	198	2671
1980	87	85	100	127	213	222	191	178	197	248	197	211	2056
1981	168	208	240	217	259	237	332	391	376	420	383	271	3502
1982	270	394	406	225	211	222	150	300	235	259	306	277	3255
1983	174	139	213	226	353	260	171	176	44	132	17	43	1948
1984	157	305	190	173	253	30	5	9	4	0	11	5	1142
1985	25	16	2	31	15	10	42	1	3	20	1	11	177
1986	12	64	11	7	6	0	5	0	1	30	6	2	144
1987	3	2	5	44	57	1	33	52	27	24	57	52	357
1988	99	12	131	127	103	152	191	114	141	179	182	208	1639
1989	143	161	179	123	202	174	170	157	176	142	157	145	1929
1990	143	154	231	168	151	139	142	160	149	224	323	278	2262
1991	240	201	244	172	206	236	231	179	246	254	197	247	2653
1992	191	241	160	157	61	87	198	188	129	207	160	143	1922
1993	49	218	183	89	110	121	23	21	58	64	55	151	1142
1994	153	21	34	6	1	7	9	45	17	16	9	18	336
1995	37	27	21	14	16	2	1	2	2	24	2	0	148
1996	2	0	1	4	6	1	20	8	0	0	28	11	81
1997	0	6	2	9	6	1	3	21	77	5	119	37	286
1998	33	16	110	69	141	68	68	122	103	80	184	194	1188
1999	201	107	113	48	161	183	199	182	92	193	203	172	1854
2000	118	171	303	181	195	193	205	135	211	148	174	229	2263
2001	174	61	176	145	132	211	71	275	211	228	262	155	2101
2002	182	189	166	218	212	75	225	286	201	220	202	147	2323
2003	112	82	98	124	89	136	187	87	73	106	118	104	1316
2004	83	53	97	56	53	41	154	111	35	86	103	40	912
2005	102	30	42	16	91	54	81	29	85	3	39	27	599
2006	10	0	6	48	2	3	7	25	5	0	15	53	174
2007	12	3	0	1	6	17	19	3	0	0	0	12	73
2008	3	0	0	2	0	0	0	0	0	0	2	1	8
2009	0	0	0	0	0	0	2	0	1	11	0	14	28
2010	28	44	9	1	8	9	10	8	9	15	25	4	170
2011	18	111	145	102	55	32	56	93	152	123	171	141	1199
2012	86	29	104	79	174	143	203	117	118	113	125	44	1335
2013	103	30	49	168	173	60	109	57	26	190	226	166	1357
2014	137	189	201	168	126	132	78	120	129	146	174	198	1798

C Monthly and yearly numbers of M-class flares 1976-2009 AD (GOES 1-14 instrumental data)

Year	Jan	Feb	Mar	Apr	May	Jun	Jul	Aug	Sep	Oct	Nov	Dec	M-Total
1976	1	1	22	5	1	1	1	3	1	1	1	2	40
1977	1	2	1	1	2	5	0	2	11	4	1	4	34
1978	2	20	8	35	27	14	36	3	16	13	9	19	202
1979	30	56	30	21	12	33	21	45	34	43	42	26	393
1980	24	16	6	35	32	44	19	18	13	31	109	38	385
1981	28	38	39	74	17	23	69	57	42	40	38	20	485
1982	25	72	27	13	27	120	106	25	7	6	48	78	554
1983	2	4	10	5	19	27	8	18	2	6	2	3	106
1984	7	26	16	36	23	0	1	1	0	0	4	0	114
1985	8	0	0	1	2	0	2	0	0	1	0	0	14
1986	3	10	2	3	1	0	0	0	0	1	0	0	20
1987	0	0	0	2	2	0	2	9	1	2	10 2	30	
1988	2	1	21	11	8	23	13	7	10	18	34	45	193
1989	95	35	88	13	45	90	8	52	65	34	58	37	620
1990	25	10	28	28	21	28	13	25	16	11	25	50	280
1991	32	52	103	41	39	66	29	33	24	53	27	91	590
1992	39	47	4	8	5	7	12	12	33	24	7	4	202
1993	2	17	13	3	5	13	4	1	2	3	3	8	74
1994	11	2	0	0	0	1	1	8	0	1	0	1	25
1995	0	5	1	2	0	0	0	0	0	3	0	0	11
1996	0	0	0	1	0	0	2	0	0	0	1	0	4
1997	0	0	0	1	1	0	0	1	6	0	11	1	21
1998	5	0	10	4	15	4	3	14	9	3	15	12	94
1999	10	6	11	5	16	17	23	23	2	8	40	9	170
2000	9	14	37	11	20	21	51	3	14	11	17	7	215
2001	10	1	37	38	11	13	3	22	50	32	46	47	310
2002	22	18	15	16	14	4	30	43	13	22	12	10	219
2003	8	3	7	14	8	41	7	4	1	37	24	6	160
2004	12	2	5	7	1	1	33	26	4	9	15	7	122
2005	21	1	0	0	13	4	19	8	26	0	7	4	103
2006	0	0	0	8	0	0	1	0	0	0	0	5	14
2007	0	0	0	0	0	10	0	0	0	0	0	0	10
2008	0	0	1	0	0	0	0	0	0	0	0	0	1
2009	0	0	0	0	0	0	0	0	0	0	0	0	0
2010	6	9	0	0	1	2	0	1	0	1	3	0	23
2011	1	13	21	3	2	2	2	7	31	8	13	8	111
2012	5	1	19	2	12	11	45	10	4	6	14	0	129
2013	5	1	3	4	14	4	1	3	0	33	19	12	99
2014	26	39	22	3	5	16	5	7	11	41	16	17	208

D Monthly and Yearly Numbers of X-Class Flares 1976-2009 AD (GOES 1-14 instrumental data)

Year	Jan	Feb	Mar	Apr	May	Jun	Jul	Aug	Sep	Oct	Nov	Dec	X-Total
1976	0	0	3	1	0	0	0	1	0	0	0	0	5
1977	0	0	0	0	0	0	0	0	1	0	0	0	1
1978	0	1	0	4	2	1	5	0	0	0	0	2	15
1979	2	5	2	1	0	3	1	4	2	2	2	1	25
1980	1	1	0	2	3	2	3	0	0	2	7	0	21
1981	1	6	1	13	3	0	5	1	1	3	1	0	35
1982	1	5	2	0	1	16	5	0	0	0	2	10	42
1983	0	1	0	0	4	1	0	0	0	0	0	0	6
1984	0	1	0	3	3	0	0	0	0	0	0	0	7
1985	1	0	0	1	0	0	0	0	0	0	0	0	2
1986	0	2	0	0	0	0	0	0	0	0	0	0	2
1987	0	0	0	0	0	0	0	0	0	0	0	0	0
1988	1	0	0	1	0	4	0	0	0	3	0	4	13
1989	7	3	12	1	2	6	1	5	6	5	9	2	59
1990	0	0	1	3	8	0	0	1	0	0	0	3	16
1991	4	1	20	1	2	6	6	2	2	5	2	3	54
1992	1	2	0	0	0	2	1	0	2	1	1	0	10
1993	0	0	0	0	0	0	0	0	0	0	0	0	0
1994	0	0	0	0	0	0	0	0	0	0	0	0	0
1995	0	0	0	0	0	0	0	0	0	0	0	0	0
1996	0	0	0	0	0	0	1	0	0	0	0	0	1
1997	0	0	0	0	0	0	0	0	0	0	3	0	3
1998	0	0	0	2	2	0	0	5	0	0	5	0	14
1999	0	0	0	0	0	0	0	2	0	1	1	0	4
2000	0	1	3	0	0	4	3	0	1	0	5	0	17
2001	0	0	1	8	0	1	0	1	1	4	2	3	21
2002	0	0	0	1	1	0	5	4	0	1	0	0	12
2003	0	0	2	0	3	4	0	0	0	7	4	0	20
2004	0	1	0	0	0	0	6	2	0	1	2	0	12
2005	6	0	0	0	0	0	2	0	10	0	0	0	18
2006	0	0	0	0	0	0	0	0	0	0	0	4	4
2007	0	0	0	0	0	0	0	0	0	0	0	0	0
2008	0	0	0	0	0	0	0	0	0	0	0	0	0
2009	0	0	0	0	0	0	0	0	0	0	0	0	0
2010	0	0	0	0	0	0	0	0	0	0	0	0	0
2011	0	1	1	0	0	0	0	1	4	0	1	0	8
2012	1	0	3	0	0	0	2	0	0	1	0	0	7
2013	0	0	0	0	4	0	0	0	0	4	4	0	12
2014	1	1	1	1	0	3	0	0	1	6	1	1	16

References

Ataç, T., Özgüç, A., 1998, *Solar Phys.* **180**, 397
Benz, A., Brajša, R., Magdalenić, J., 2007, *Solar Phys.* **240**, 263
Bonev, B., Penev, K., Sello, S., 2004, *ApJ* **605**, L81
Cheng, X., Ding, M. D., Zhang, J., 2010a, *ApJ* **712**, 1302
Cheng, X., Zhang, J., Ding, M. D. Poomvises, W., 2010b, *ApJ* **712**, 752
Gosling, J. T., 1993, *J. Geophys. Res.* **98**, 18937
Hoyt, D. V. and Schatten, K. H., 1998, *Solar Phys.* **181**, 491
Huang, J., Yan, Y. H., Liu, Y. Y., 2008, *Solar Phys.* **253**, 143
Kane, R. P., 2009, *Solar Phys.* **255**, 163
Kiliç, H., 2009, *Solar Phys.* **255**, 155
Kim, Yeon-Han, Bong, Su-Chan, Park, Y.-D. et al., 2009, *ApJ* **705**, 1721
Knoška, S., Petrásek, J., 1984, *Contrib. Astron. Obs. Skalnat? Pleso* **12**, 165
Komitov, B., 1997, *Bulg. Geophys. J.* **23**, 69
Komitov, B. and Kaftan, V., 2003, *Geomagn. & Aeronomy* **43**, 553
Komitov, B., Duchlev, P., Koleva, K., et al., 2010, ArXiv e-prints, 1007.2735
Link, F., Kleczek, J., 1949, *Bull. Astron. Inst. Czechosl.* **1**, 69
Lobzin, V. V., Cairns, I. H., Robinson, P. A. et al., 2010, *ApJ* **710**, L58
Neupert, W. M., 2011, *Solar Phys.* **272**, 319
Reames, D. V., 2004, *Adv.Space Res.* **34**, 381
Shanmugaraju, A., Moon, Y.-J., Dryer, M. et al., 2003, *Solar Phys.* **217**, 301
Shibata, K., 1999, *Astrophys. Space Sci.* **264**, 129
Sterling, A. C., Hudson, H. S., Thompson, B. J. et al., 2000, *ApJ* **532**, 628
Tripathi, D., Bothmer, V., Cremades, H., 2004, *A&A* **422**, 337
Vernova, E. S., Tyasto, M. I., Baranov, D. G., 2005, *Mem. Soc. Astr. It.* **76**, 1052
Vernova, E. S., Mursula, K., Tyasto, M. I., Baranov, D. G., 2002, *Solar Phys.* **205**, 371
Webb, D. F., Forbes, T. G., Aurass, H. et al., 1994, *Solar Phys.* **153**, 73
White, S. M., Thomas, R. J., Schwartz, R. A. et al., 2005, *Solar Phys.* **227**, 231